Isovector axial vector form factor of the nucleon from lattice QCD with improved Wilson fermions

Konstantin Ottnad[a]

in collaboration with

Dalibor Djukanovic[b], Jonna Koponen[b], Harvey Meyer[a,b], Tobias Schulz[a], Georg von Hippel[a], Hartmut Wittig[a,b]

[a] Institut für Kernphysik, Johannes Gutenberg-Universität Mainz
[b] Helmholtz-Institut Mainz, Johannes Gutenberg-Universität Mainz

Interdisciplinary Developments in Neutrino Physics,
KITP @ UC Santa Barbara, Mar 28-31, 2022

JOHANNES GUTENBERG UNIVERSITÄT MAINZ

JG|U

HIM Helmholtz-Institut Mainz

PRISMA+

erc European Research Council Established by the European Commission

Introduction

- Experimental knowledge on axial form factors is limited as νN interactions are difficult to measure.
- νN required for neutrino-nucleus cross section which are input for upcoming neutrino experiments.
- LQCD can be used to compute axial form factor.
- Lattice calulcations are already competitive in terms of errors.

$\Rightarrow$ **LQCD can provide crucial input to future neutrino experiments.**

- Going beyond dedicated studies of g_A and r_A, LQCD can provide a parametrization of the physical form factor for $0 \leq Q^2 \lesssim 1\,\mathrm{GeV}^2$.
- While recent calculations for g_A agree with experiment, situation is much less clear for r_A (and FF itself).

Reliable and precise determination of the physical form factor remains a challenging task.

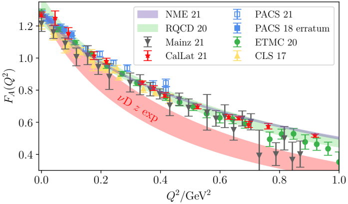

Figure taken from **A. S. Meyer et al., arXiv:2201.01839**

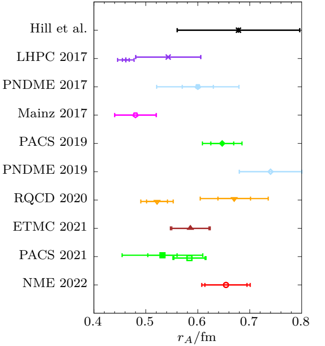

Mainz nucleon structure program

- **Isovector nucleon charges $g_{A,S,T}^{u-d}$** and twist-2 matrix elements *PRD 100 (2019) 3, 034513*
  → update of 2019 analysis in progress. *POS Lattice 2021, arXiv:2110.10500*
- Isovector electromagnetic form factors $G_E^{u-d}(Q^2)$ and $G_M^{u-d}(Q^2)$ *PRD 103 (2021) 9, 094522*
- **Isovector axial form factor** (not yet published, $N_f = 2+1$ analysis ongoing) *POS Lattice 2021, arXiv:2112.00127*
  → Analysis carried out by Jonna Koponen and Tobias Schulz
- Isoscalar contributions (involving quark-disconnected diagrams)
  - Strange electromagnetic form factor *PRL 123 (2019) 21, 212001*
  - Electromagnetic form factors (analysis ongoing) *POS Lattice 2021, arXiv:2110.10626*
  - Charges / further form factors, σ-term etc. ...

Results shown in this talk are preliminary!

Lattice calculation

Extraction of axial FF requires ratio to cancel unknown overlap factors in 3pt function

$$R_{\mathcal{O}}(\vec{q}, t_{\rm sep}, t_{\rm ins}) = \frac{C^{\rm 3pt}_{\mathcal{O}}(\vec{q}, t_{\rm sep}, t_{\rm ins})}{C^{\rm 2pt}(\vec{0}, t_{\rm sep})} \sqrt{\frac{C^{\rm 2pt}(-\vec{q}, t_{\rm sep} - t_{\rm ins}) C^{\rm 2pt}(\vec{0}, t_{\rm ins}) C^{\rm 2pt}(\vec{0}, t_{\rm sep})}{C^{\rm 2pt}(\vec{0}, t_{\rm sep} - t_{\rm ins}) C^{\rm 2pt}(-\vec{q}, t_{\rm ins}) C^{\rm 2pt}(-\vec{q}, t_{\rm sep})}}.$$

Two possible choices for axial vector current insertion

$$R_{A_0}(\vec{q}, t_{\rm sep}, t_{\rm ins}) = \frac{q_3}{\sqrt{2E(E+m_N)}} \left(G_A(Q^2) + \frac{m_N - E}{2m_N} G_P(Q^2) \right),$$

$$R_{A_k}(\vec{q}, t_{\rm sep}, t_{\rm ins}) = \frac{i}{\sqrt{2E(E+m_N)}} \left((m_N + E) G_A(Q^2) \delta_{3k} - \frac{q_3 q_k}{2m_N} G_P(Q^2) \right).$$

Consider effective form factor from spatial insertion

$$\boxed{G_A^{\rm eff}(\vec{q}, t_{\rm sep}, t_{\rm ins}) = \frac{-i(E - m_N)}{f(q^2)} \sum_{k=1}^{3} \frac{\delta_{3k} - q_3 q_k / \vec{q}^2}{q_1^2 + q_2^2} R_{A_k}(\vec{q}, t_{\rm sep}, t_{\rm ins})}, \qquad f(q^2) = \frac{1}{2E\sqrt{E + m_N}}.$$

Remarks:

- Much stronger excited state contamination for A_0 due to $N\pi$ states.
- A_0 required for checking PCAC but not for extracting axial FF itself.

Lattice calculation

Need to compute 2pt and 3pt functions:

- For 3pt functions we use sequential inversions through the sink, setting $p' = 0$.
- Only quark-connected 3pt functions for isovector NMEs.
- Full non-perturbative renormalization available for g_A.
  Eur.Phys.J.C 79 (2019) 1, 23
- Use of improved current for 3pt function
  $\rightarrow$ leading lattice artifact of $\mathcal{O}(a^2)$

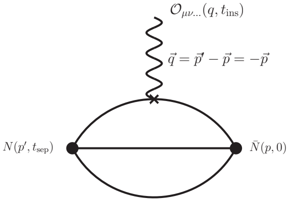

Truncated solver method gives speedup of a factor 2-5

Comput.Phys.Commun. 181 (2010) 1570-1583
PRD 91 (2015) no.11, 114511

$$\langle \mathcal{O} \rangle = \left\langle \frac{1}{N_{LP}} \sum_{i=1}^{N_{LP}} \mathcal{O}_n^{LP} \right\rangle + \langle \mathcal{O}_{\rm bias} \rangle \,, \quad \mathcal{O}_{\rm bias} = \frac{1}{N_{HP}} \sum_{i=1}^{N_{HP}} (\mathcal{O}_n^{HP} - \mathcal{O}_n^{LP}) \,.$$

- Use as many point-to-all propagators as possible / affordable.
- Actual source setup depends on source-sink separation $t_{\rm sep}$ and boundary conditions.

Ensembles and setup details

ID	a/fm	T/a	L/a	$M_\pi\,/\,\mathrm{MeV}$	$M_\pi L$	N_{conf}	N_{meas}	$t_{\mathrm{sep}}^{\mathrm{lo}}\,/\,\mathrm{fm}$	$t_{\mathrm{sep}}^{\mathrm{hi}}\,/\,\mathrm{fm}$	$N_{t_{\mathrm{sep}}}$
C101	0.086	96	48	0.225	4.73	2000	64000	0.35	1.47	14
N101		128	48	0.282	5.91	1596	51072			
H105		96	32	0.281	3.93	1027	49296			
H102		96	32	0.354	4.96	2005	32080			
D450	0.076	128	64	0.216	5.35	500	64000	0.31	1.53	9
N451		128	48	0.286	5.31	1011	129408			
S400		128	32	0.350	4.33	2873	45968			
E250	0.064	192	96	0.130	4.06	400	102400	0.26	1.41	10
D200		128	64	0.202	4.22	2000	64000			
N200		128	48	0.281	4.39	1712	20544			
S201		128	32	0.292	3.05	2093	66976			
N203		128	48	0.345	5.41	1543	24688			
E300	0.050	192	96	0.173	4.20	570	18240	0.20	1.40	13
J303		192	64	0.260	4.19	1073	17168			
N302		128	48	0.349	4.22	2201	35216			

- Gauge configurations generated by the "Coordinated lattice simulations" (CLS) consortium.
- $N_f = 2+1$ flavors of non-perturbatively improved Wilson clover fermions. *JHEP 1502 (2015) 043*
- N_{conf} and N_{meas} are target numbers, production not entirely complete / available statistics not yet fully included in analysis.

Ensembles and setup details

ID	a/fm	T/a	L/a	M_π / MeV	$M_\pi L$	N_{conf}	N_{meas}	$t_{\text{sep}}^{\text{lo}}$ / fm	$t_{\text{sep}}^{\text{hi}}$ / fm	$N_{t\text{sep}}$
C101	**0.086**	96	48	0.225	4.73	2000	64000	0.35	1.47	14
N101		128	48	0.282	5.91	1596	51072			
H105		96	32	0.281	3.93	1027	49296			
H102		96	32	0.354	4.96	2005	32080			
D450	**0.076**	128	64	0.216	5.35	500	64000	0.31	1.53	9
N451		128	48	0.286	5.31	1011	129408			
S400		128	32	0.350	4.33	2873	45968			
E250	**0.064**	192	96	0.130	4.06	400	102400	0.26	1.41	10
D200		128	64	0.202	4.22	2000	64000			
N200		128	48	0.281	4.39	1712	20544			
S201		128	32	0.292	3.05	2093	66976			
N203		128	48	0.345	5.41	1543	24688			
E300	**0.050**	192	96	0.173	4.20	570	18240	0.20	1.40	13
J303		192	64	0.260	4.19	1073	17168			
N302		128	48	0.349	4.22	2201	35216			

- **Ensembles cover four values of the lattice spacing a**
  $\rightarrow$ continuum extrapolation
- Many different physical volumes with $L \approx 2 \ldots 6\,\text{fm}$, typically $M_\pi L > 4$.
  $\rightarrow$ extrapolation to infinite volume / check for finite size effects.
- Pion masses from $\sim 130\,\text{MeV}$ to $\sim 350\,\text{MeV}$
  $\rightarrow$ chiral extrapolation and checking its convergence
- Two very large and fine boxes at (near) physical quark mass.

Ensembles and setup details

ID	a/fm	T/a	L/a	M_π / MeV	$M_\pi L$	N_{conf}	N_{meas}	$t_{\text{sep}}^{\text{lo}}$ / fm	$t_{\text{sep}}^{\text{hi}}$ / fm	$N_{t\text{sep}}$
C101	0.086	96	48	0.225	**4.73**	2000	64000	0.35	1.47	14
N101		128	48	0.282	**5.91**	1596	51072			
H105		96	32	0.281	**3.93**	1027	49296			
H102		96	32	0.354	**4.96**	2005	32080			
D450	0.076	128	64	0.216	**5.35**	500	64000	0.31	1.53	9
N451		128	48	0.286	**5.31**	1011	129408			
S400		128	32	0.350	**4.33**	2873	45968			
E250	0.064	192	96	0.130	**4.06**	400	102400	0.26	1.41	10
D200		128	64	0.202	**4.22**	2000	64000			
N200		128	48	0.281	**4.39**	1712	20544			
S201		128	32	0.292	**3.05**	2093	66976			
N203		128	48	0.345	**5.41**	1543	24688			
E300	0.050	192	96	0.173	**4.20**	570	18240	0.20	1.40	13
J303		192	64	0.260	**4.19**	1073	17168			
N302		128	48	0.349	**4.22**	2201	35216			

- Ensembles cover four values of lattice spacing
  → continuum extrapolation
- **Many different lattice volumes with $L \approx 2 \ldots 6\,\text{fm}$, typically $M_\pi L > 4$.**
  → extrapolation to infinite volume / check for finite size effects.
- Pion masses from $\sim 130\,\text{MeV}$ to $\sim 350\,\text{MeV}$
  → chiral extrapolation and checking its convergence
- Two very large and fine boxes at (near) physical quark mass.

Ensembles and setup details

ID	a/fm	T/a	L/a	M_π / MeV	$M_\pi L$	N_{conf}	N_{meas}	$t_{\mathrm{sep}}^{\mathrm{lo}}$ / fm	$t_{\mathrm{sep}}^{\mathrm{hi}}$ / fm	$N_{t_{\mathrm{sep}}}$
C101	0.086	96	48	**0.225**	4.73	2000	64000	0.35	1.47	14
N101		128	48	**0.282**	5.91	1596	51072			
H105		96	32	**0.281**	3.93	1027	49296			
H102		96	32	**0.354**	4.96	2005	32080			
D450	0.076	128	64	**0.216**	5.35	500	64000	0.31	1.53	9
N451		128	48	**0.286**	5.31	1011	129408			
S400		128	32	**0.350**	4.33	2873	45968			
E250	0.064	192	96	**0.130**	4.06	400	102400	0.26	1.41	10
D200		128	64	**0.202**	4.22	2000	64000			
N200		128	48	**0.281**	4.39	1712	20544			
S201		128	32	**0.292**	3.05	2093	66976			
N203		128	48	**0.345**	5.41	1543	24688			
E300	0.050	192	96	**0.173**	4.20	570	18240	0.20	1.40	13
J303		192	64	**0.260**	4.19	1073	17168			
N302		128	48	**0.349**	4.22	2201	35216			

- Ensembles cover four values of lattice spacing
  $\rightarrow$ continuum extrapolation
- Many different lattice volumes with $L \approx 2 \dots 6\,\mathrm{fm}$, typically $M_\pi L > 4$.
  $\rightarrow$ extrapolation to infinite volume / check for finite size effects.
- **Pion masses from** $\sim 130\,\mathrm{MeV}$ **to** $\sim 350\,\mathrm{MeV}$
  $\rightarrow$ chiral extrapolation and checking its convergence
- Two very large and fine boxes at (near) physical quark mass.

Ensembles and setup details

ID	a/fm	T/a	L/a	$M_\pi\,/\,\mathrm{MeV}$	$M_\pi L$	N_{conf}	N_{meas}	$t_{\mathrm{sep}}^{\mathrm{lo}}\,/\,\mathrm{fm}$	$t_{\mathrm{sep}}^{\mathrm{hi}}\,/\,\mathrm{fm}$	$N_{t_{\mathrm{sep}}}$
C101	0.086	96	48	0.225	4.73	2000	64000	0.35	1.47	14
N101		128	48	0.282	5.91	1596	51072			
H105		96	32	0.281	3.93	1027	49296			
H102		96	32	0.354	4.96	2005	32080			
D450	0.076	128	64	0.216	5.35	500	64000	0.31	1.53	9
N451		128	48	0.286	5.31	1011	129408			
S400		128	32	0.350	4.33	2873	45968			
E250	0.064	192	96	0.130	4.06	400	102400	0.26	1.41	10
D200		128	64	0.202	4.22	2000	64000			
N200		128	48	0.281	4.39	1712	20544			
S201		128	32	0.292	3.05	2093	66976			
N203		128	48	0.345	5.41	1543	24688			
E300	0.050	192	96	0.173	4.20	570	18240	0.20	1.40	13
J303		192	64	0.260	4.19	1073	17168			
N302		128	48	0.349	4.22	2201	35216			

- Ensembles cover four values of lattice spacing
  $\rightarrow$ continuum extrapolation
- Many different lattice volumes with $L \approx 2 \ldots 6\,\mathrm{fm}$, typically $M_\pi L > 4$.
  $\rightarrow$ extrapolation to infinite volume / check for finite size effects.
- Pion masses from $\sim 130\,\mathrm{MeV}$ to $\sim 350\,\mathrm{MeV}$
  $\rightarrow$ chiral extrapolation and checking its convergence
- **Two very large and fine boxes at (near) physical quark mass.**

Ensembles and setup details

ID	a/fm	T/a	L/a	M_π / MeV	$M_\pi L$	$N_{\rm conf}$	$N_{\rm meas}$	$t_{\rm sep}^{\rm lo}$ / fm	$t_{\rm sep}^{\rm hi}$ / fm	$N_{t_{\rm sep}}$
C101	0.086	96	48	0.225	4.73	2000	64000	**0.35**	**1.47**	**14**
N101		128	48	0.282	5.91	1596	51072			
H105		96	32	0.281	3.93	1027	49296			
H102		96	32	0.354	4.96	2005	32080			
D450	0.076	128	64	0.216	5.35	500	64000	**0.31**	**1.53**	**9**
N451		128	48	0.286	5.31	1011	129408			
S400		128	32	0.350	4.33	2873	45968			
E250	0.064	192	96	0.130	4.06	400	102400	**0.26**	**1.41**	**10**
D200		128	64	0.202	4.22	2000	64000			
N200		128	48	0.281	4.39	1712	20544			
S201		128	32	0.292	3.05	2093	66976			
N203		128	48	0.345	5.41	1543	24688			
E300	0.050	192	96	0.173	4.20	570	18240	**0.20**	**1.40**	**13**
J303		192	64	0.260	4.19	1073	17168			
N302		128	48	0.349	4.22	2201	35216			

- **Large number of source-sink separations available, typically $t_{\rm sep} \approx 0.3 \ldots 1.5\,{\rm fm}$.**
- $N_{\rm meas}$ reduced by factor of two in steps of $\Delta t_{\rm sep} \approx 0.2\,{\rm fm}$ for $t_{\rm sep} < 1\,{\rm fm}$.
  $\rightarrow$ Signal-to-noise ratio as function of $t_{\rm sep}$ closer to constant
- On lattices with periodic boundary conditions and some other (newer) runs this scaling of statistics has been performed beyond $t_{\rm sep} = 1\,{\rm fm}$ up to $t_{\rm sep}^{\rm hi}$.

Ensembles and setup details

ID	a/fm	T/a	L/a	M_π / MeV	$M_\pi L$	N_{conf}	N_{meas}	$t_{\mathrm{sep}}^{\mathrm{lo}}$ / fm	$t_{\mathrm{sep}}^{\mathrm{hi}}$ / fm	$N_{t_{\mathrm{sep}}}$
C101	0.086	96	48	0.225	4.73	2000	**64000**	**0.35**	**1.47**	**14**
N101		128	48	0.282	5.91	1596	**51072**			
H105		96	32	0.281	3.93	1027	**49296**			
H102		96	32	0.354	4.96	2005	**32080**			
D450	0.076	128	64	0.216	5.35	500	**64000**	**0.31**	**1.53**	**9**
N451		128	48	0.286	5.31	1011	**129408**			
S400		128	32	0.350	4.33	2873	**45968**			
E250	0.064	192	96	0.130	4.06	400	**102400**	**0.26**	**1.41**	**10**
D200		128	64	0.202	4.22	2000	**64000**			
N200		128	48	0.281	4.39	1712	**20544**			
S201		128	32	0.292	3.05	2093	**66976**			
N203		128	48	0.345	5.41	1543	**24688**			
E300	0.050	192	96	0.173	4.20	570	**18240**	**0.20**	**1.40**	**13**
J303		192	64	0.260	4.19	1073	**17168**			
N302		128	48	0.349	4.22	2201	**35216**			

- Large number of source-sink separations available, typically $t_{\mathrm{sep}} \approx 0.3 \ldots 1.5\,\mathrm{fm}$.
- **N_{meas} reduced by factor of two in steps of $\Delta t_{\mathrm{sep}} \approx 0.2\,\mathrm{fm}$ for $t_{\mathrm{sep}} < 1\,\mathrm{fm}$.**
  $\to$ **Signal-to-noise ratio as function of t_{sep} closer to a constant.**
- On lattices with periodic boundary conditions and some other (newer) runs this scaling of statistics has been performed beyond $t_{\mathrm{sep}} = 1\,\mathrm{fm}$ up to $t_{\mathrm{sep}}^{\mathrm{hi}}$.

Ensembles and setup details

ID	a/fm	T/a	L/a	M_π / MeV	$M_\pi L$	N_{conf}	N_{meas}	$t_{\mathrm{sep}}^{\mathrm{lo}}$ / fm	$t_{\mathrm{sep}}^{\mathrm{hi}}$ / fm	$N_{t_{\mathrm{sep}}}$
C101	0.086	96	48	0.225	4.73	2000	64000	0.35	1.47	14
N101		128	48	0.282	5.91	1596	51072			
H105		96	32	0.281	3.93	1027	49296			
H102		96	32	0.354	4.96	2005	32080			
D450	0.076	128	64	0.216	5.35	500	64000	0.31	1.53	9
N451		128	48	0.286	5.31	1011	129408			
S400		128	32	0.350	4.33	2873	45968			
E250	0.064	192	96	0.130	4.06	400	102400	0.26	1.41	10
D200		128	64	0.202	4.22	2000	64000			
N200		128	48	0.281	4.39	1712	20544			
S201		128	32	0.292	3.05	2093	66976			
N203		128	48	0.345	5.41	1543	24688			
E300	0.050	192	96	0.173	4.20	570	18240	0.20	1.40	13
J303		192	64	0.260	4.19	1073	17168			
N302		128	48	0.349	4.22	2201	35216			

- Large number of source-sink separations available, typically $t_{\mathrm{sep}} \approx 0.3 \ldots 1.5\,\mathrm{fm}$.
- N_{meas} reduced by factor of two in steps of $\Delta t_{\mathrm{sep}} \approx 0.2\,\mathrm{fm}$ for $t_{\mathrm{sep}} < 1\,\mathrm{fm}$.
  $\rightarrow$ Signal-to-noise ratio as function of t_{sep} closer to constant
- On lattices with periodic boundary conditions and some other (newer) runs scaling of statistics has been performed beyond $t_{\mathrm{sep}} = 1\,\mathrm{fm}$ up to $t_{\mathrm{sep}}^{\mathrm{hi}}$.

Isovector axial charge g_A^{u-d}

The isovector axial charge g_A^{u-d} is a benchmark observable for lattice QCD nucleon structure calculations:

- Data for g_A^{u-d} statistically most precise (apart from el.-mag FF).
- Requires careful treatment of **excited states** and controlled **physical extrapolation** (i.e. chiral, continuum and infinite volume extrapolation).
- Our analysis is performed simultaneously for six NMEs at $Q^2 = 0$, i.e.

1. for **local** operators ($\rightarrow g_A^{u-d}, g_S^{u-d}, g_T^{u-d}$)

$$\mathcal{O}_\mu^A = \bar{q}\gamma_\mu\gamma_5 q, \quad \mathcal{O}^S = \bar{q}q, \quad \mathcal{O}_{\mu\nu}^T = \bar{q}i\sigma_{\mu\nu}q\,.$$

2. for **one-derivate, dimension-four** operators ($\rightarrow \langle x\rangle_{u-d}, \langle x\rangle_{\Delta u-\Delta d}, \langle x\rangle_{\delta u-\delta d}$)

$$\mathcal{O}_{\mu\nu}^{vD} = \bar{q}\gamma_{\{\mu}\overleftrightarrow{D}_{\nu\}}\,q\,, \quad \mathcal{O}_{\mu\nu}^{aD} = \bar{q}\gamma_{\{\mu}\gamma_5\overleftrightarrow{D}_{\nu\}}\,q\,, \quad \mathcal{O}_{\mu\nu\rho}^{tD} = \bar{q}\sigma_{[\mu\{\nu]}\overleftrightarrow{D}_{\rho\}}\,q\,,$$

$Q^2 = 0$ NMEs are obtained from simplified ratio

$$R^{\mathcal{O}}_{\mu_1,\dots,\mu_n}(t_{\rm sep}, t_{\rm ins}) = \frac{C^{\mathcal{O},3\rm pt}_{\mu_1,\dots\mu_n}(\vec{q}=0, t_{\rm sep}, t_{\rm ins})}{C^{2\rm pt}(\vec{q}=0, t_{\rm sep})}\,.$$

$\rightarrow$ **Extraction of groundstate from data at $t_{\rm sep} \lesssim 1.5\,\mathrm{fm}$ requires dedicated analysis.**

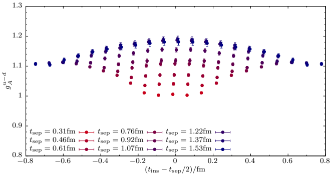

Methods for groundstate extraction

1. Plateau / midpoint method (not used):
   - Simply use ratio value at a given (large) $t_{\rm sep}$ and $t_{\rm ins} = t_{\rm sep}/2$.
   - Residual excited state corrections $\sim e^{-\Delta t_{\rm sep}/2}$, with typical energy gap $\Delta \approx 2M_\pi$

$\Rightarrow$ Generally insufficient suppression of excited states.

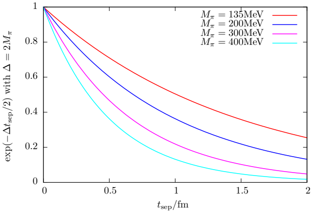

Methods for groundstate extraction

1. Plateau / midpoint method (not used):
   - Simply use ratio value at a given (large) $t_{\rm sep}$ and $t_{\rm ins} = t_{\rm sep}/2$.
   - Residual excited state corrections $\sim e^{-\Delta t_{\rm sep}/2}$, with typical energy gap $\Delta \approx 2M_\pi$

$\Rightarrow$ Generally insufficient suppression of excited states.

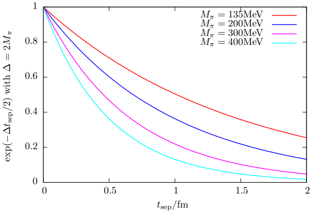

2. Two-state fits (used for g_A in 2019 publication)

$$R(t_{\rm ins}, t_{\rm sep}) = M_{00} + a_0(e^{-\Delta t_{\rm ins}} - e^{-\Delta(t_{\rm sep}-t_{\rm ins})}) + a_1 e^{-\Delta t_{\rm sep}}$$

   - Explicitly account for leading correction.
   - Demanding $M_\pi t_{\rm ins}^{\rm min} \gtrsim 0.5$ at $M_\pi = 135\,\mathrm{MeV}$ implies $t_{\rm sep}^{\rm min} \approx 1.5\,\mathrm{fm}$

$\Rightarrow$ Insufficient for $M_\pi \lesssim 200\,\mathrm{MeV}$.

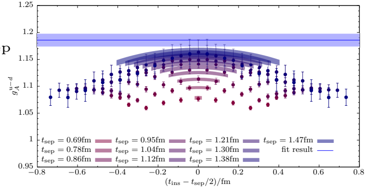

Methods for groundstate extraction

1. Plateau / midpoint method (not used):
   - Simply use ratio value at a given (large) $t_{\rm sep}$ and $t_{\rm ins} = t_{\rm sep}/2$.
   - Residual excited state corrections $\sim e^{-\Delta t_{\rm sep}/2}$, with typical energy gap $\Delta \approx 2M_\pi$

   $\Rightarrow$ Generally insufficient suppression of excited states.

2. Two-state fits (used for g_A in 2019 publication)

   $$R(t_{\rm ins}, t_{\rm sep}) = M_{00} + a_0(e^{-\Delta t_{\rm ins}} - e^{-\Delta(t_{\rm sep} - t_{\rm ins})}) + a_1 e^{-\Delta t_{\rm sep}}$$

   - Explicitly account for leading correction.
   - Demanding $M_\pi t_{\rm ins}^{\rm min} \gtrsim 0.5$ at $M_\pi = 135\,\mathrm{MeV}$ implies $t_{\rm sep}^{\rm min} \approx 1.5\,\mathrm{fm}$

   $\Rightarrow$ Insufficient for $M_\pi \lesssim 200\,\mathrm{MeV}$.

3. **Summation method (used here)**

   $$\sum_{t=a}^{t_{\rm sep}-a} R(t_{\rm ins}, t_{\rm sep}) = \mathrm{const} + M_{00}(t_{\rm sep} - a) + \mathcal{O}(e^{-\Delta t_{\rm sep}})$$

   - **Favorable correction $\sim e^{-\Delta t_{\rm sep}}$ vs. $\sim e^{-\Delta t_{\rm ins}}$.**
   - Can be extended to include higher states ...

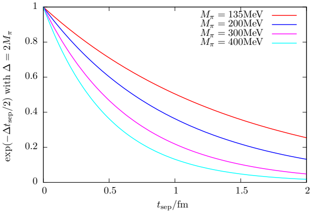

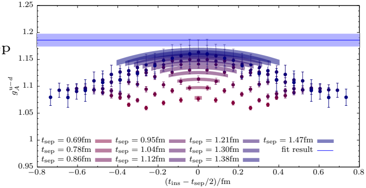

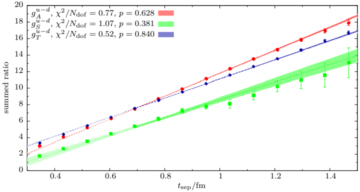

Two-state truncation for summation method

Two-state truncation of the summed ratio $S(t_{\rm sep}) = \sum_{t_{\rm ins}=a}^{t_{\rm sep}-a} R(t_{\rm ins}, t_{\rm sep})$

$$S(t_{\rm sep}) = M_{00}\left(1 - \frac{|A_1|^2}{|A_0|^2} e^{-\Delta t_{\rm sep}}\right)(t_{\rm sep} - a) + 2M_{01}\,\mathrm{Re}\left[\frac{A_1}{A_0}\right] \frac{e^{-\Delta a} - \left(1 + \frac{|A_1|^2}{|A_0|^2} e^{-\Delta a}\right) e^{-\Delta t_{\rm sep}}}{1 - e^{-\Delta a}}$$
$$+ M_{11}\frac{|A_1|^2}{|A_0|^2} e^{-\Delta t_{\rm sep}}(t_{\rm sep} - a) + \mathcal{O}(e^{-2\Delta t_{\rm sep}}),$$

- M_{ij} parameters denote matrix elements.
- Δ is the leading energy gap.
- $A_{0,1}$ are amplitudes of the two-point function.

Redefining M_{01}, M_{11} to absorb ambiguous terms yields:

$$S(t_{\rm sep}) = M_{00}(t_{\rm sep} - a) + 2\tilde{M}_{01} \frac{e^{-\Delta a} - \left(1 + \frac{|A_1|^2}{|A_0|^2} e^{-\Delta a}\right) e^{-\Delta t_{\rm sep}}}{1 - e^{-\Delta a}} + \tilde{M}_{11} e^{-\Delta t_{\rm sep}}(t_{\rm sep} - a) + \mathcal{O}(e^{-2\Delta t_{\rm sep}}).$$

NOTE: Terms $\sim \frac{|A_1|^2}{|A_0|^2}$ are not constrained at our level of statistics and not included in the final fit model.

Fit models

1. Plain summation method fits to individual observables:

$$S(t_{\rm sep}) = {\rm const} + M_{00}(t_{\rm sep} - a)\,.$$

2. Simultaneous two-state summmation method fits **(our preferred model)**:

$$S(t_{\rm sep}) = M_{00}(t_{\rm sep} - a) + 2\tilde{M}_{01}\,\frac{e^{-\Delta a} - e^{-\Delta t_{\rm sep}}}{1 - e^{-\Delta a}}\,.$$

- Fits are performed **simultaneously** for $g_{A,S,T}^{u-d}$ and $\langle x\rangle_{u-d}$, $\langle x\rangle_{\Delta u-\Delta d}$, $\langle x\rangle_{\delta u-\delta d}$.
- We have also tested another variation of the two-state model

$$S(t_{\rm sep}) = c_0 + c_1(t_{\rm sep} - a) + c_2 e^{-\Delta t_{\rm sep}} + c_3(t_{\rm sep} - a)e^{-\Delta t_{\rm sep}}\,,$$

where $c_1 = M_{00}$ and c_0 receives contributions from all higher states (similar to the constant term in the plain summation method).

Features of summation method based fits

- Results only depend on choice of $t_{\mathrm{sep}}^{\mathrm{min}}$.
- No need for priors.
- Six observables are fitted simultaneously for the two-state summation method (similar to ratio fits):

$\Rightarrow$ **Correlation helps to reduce errors.**

- Dimension of covariance matrix (much) smaller than for ratio based fits at common $t_{\mathrm{sep}}^{\mathrm{min}}$.

$\Rightarrow$ **Simultanous two-state summation fits are more stable than ratio fits!**

- For a common choice of $t_{\mathrm{sep}}^{\mathrm{min}}$ the two-state summation fits have a **favorable, leading correction**

$$\sim e^{-\Delta t_{\mathrm{sep}}^{\mathrm{min}}}$$

compared to the ratio-based two-state fits:

$$\sim e^{-\Delta t_{\mathrm{ins}}^{\mathrm{min}}} = e^{-\Delta t_{\mathrm{sep}}^{\mathrm{min}}/2}$$

Plain vs simultaneous two-state summation method (local NMEs)

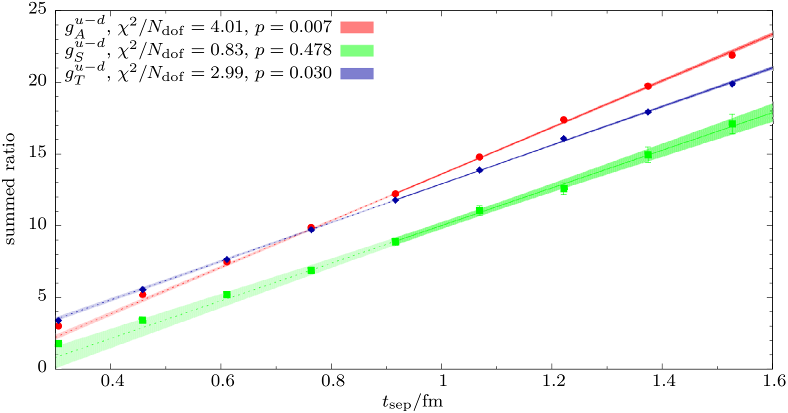

Plain summation method fits for local operator insertions on N451 ensemble ($M_\pi = 286\,\mathrm{MeV}$, $a \approx 0.076\,\mathrm{fm}$).

- Deviation from linear behavior at small values of t_{sep}.
- Observables are fitted independently.

Plain vs simultaneous two-state summation method (local NMEs)

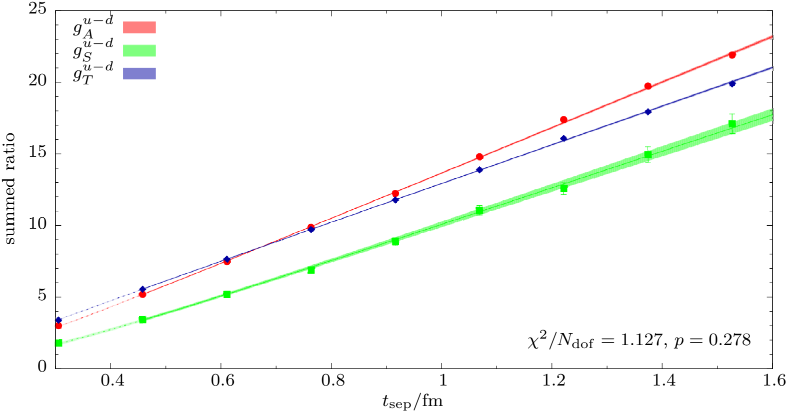

Simultaneous two-state summation method fits for local operator insertions on N451 ensemble ($M_\pi = 286\,\mathrm{MeV}$, $a \approx 0.076\,\mathrm{fm}$).

- Data described well by two-state fit to much smaller t_{sep}.
- **All six observables are fitted simultaneously.**

Plain vs simultaneous two-state summation method (twist-2 NMEs)

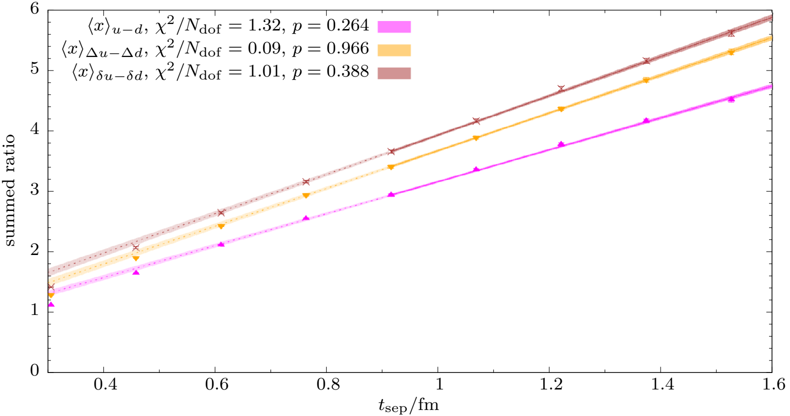

Plain summation method fits for twist-2 operator insertions on N451 ensemble ($M_\pi = 286\,\mathrm{MeV}$, $a \approx 0.076\,\mathrm{fm}$).

- Again, deviation from linear behavior at small values of t_{sep}.

Plain vs simultaneous two-state summation method (twist-2 NMEs)

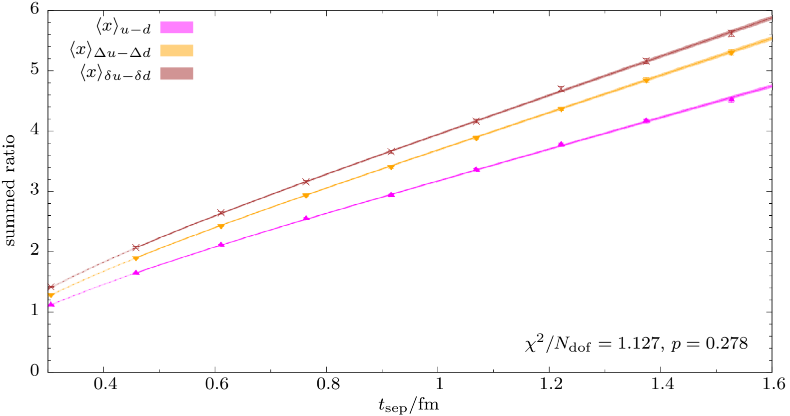

Simultaneous two-state summation method fits for twist-2 operator insertions on N451 ensemble ($M_\pi = 286\,\mathrm{MeV}$, $a \approx 0.076\,\mathrm{fm}$).

- Again, data described very well by the two-state fit.
- However, the fit quality deteriorates drastically if further decreasing $t_{\rm sep}$!

Convergence of single- and two-state summation method for g_A^{u-d}

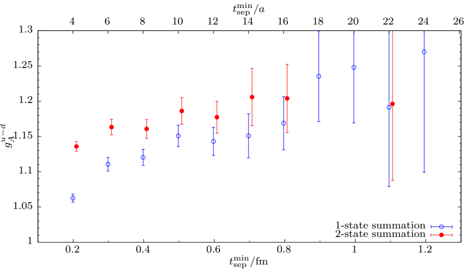

E300 $M_\pi = 172\,\mathrm{MeV}$, $a = 0.050\,\mathrm{fm}$

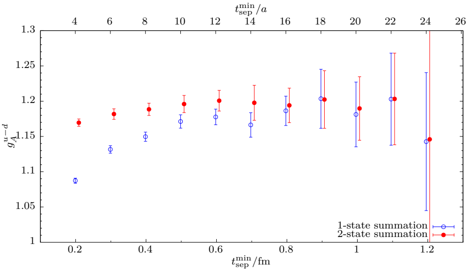

J303 $M_\pi = 260\,\mathrm{MeV}$, $a = 0.050\,\mathrm{fm}$

- Plain summation and two-state fits converge.
- Two-state fit allows to include smaller t_{sep}.
- Plain summation fits:
  Choose $M_\pi t_{\mathrm{sep}}^{\mathrm{min}} \geq 0.7$ and $t_{\mathrm{sep}}^{\mathrm{min}} \geq 0.5\,\mathrm{fm}$.
- Two-state fits:
  Choose $M_\pi t_{\mathrm{sep}}^{\mathrm{min}} \geq 0.5$.

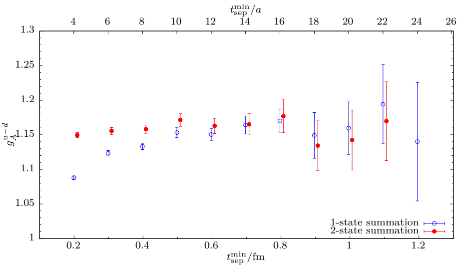

N302 $M_\pi = 349\,\mathrm{MeV}$, $a = 0.050\,\mathrm{fm}$

Physical extrapolation – CCF fit models

We consider the following ansatz for the chiral, continuum and finite volume extrapolation inspired by the NNLO chiral expansion of g_A

JHEP 04 (1999) 031

$$\boxed{g_A^{u-d}(M_\pi, a, L) = A + BM_\pi^2 + CM_\pi^2 \log M_\pi + DM_\pi^3 + Ea^2 + F\frac{M_\pi^2}{\sqrt{M_\pi L}}e^{-M_\pi L}\,,}$$

where

- $A = \mathring{g}_A$, B, D E and F are free fit parameters.
- C is known analytically, i.e. $C = \frac{-\mathring{g}_A}{(2\pi f_\pi)^2}\left(1 + 2\mathring{g}_A^2\right)$.

Remarks:

- An NLO fit including the chiral log imposes a curvature not observed in the data.
- An NLO fit with a free parameter C gives the “wrong” sign.

We employ two fit models for g_A^{u-d}:

1. NLO fit without a chiral log: $g_A^{u-d}(M_\pi, a, L) = A + BM_\pi^2 + Ea^2 + F\frac{M_\pi^2}{\sqrt{M_\pi L}}e^{-M_\pi L}$.
2. **Full NNLO fit as given above.**

We use t_0 to set the scale, with $\sqrt{8t_0^{\mathrm{phys}}} = 0.415(4)_{\mathrm{stat}}(2)_{\mathrm{sys}}\,\mathrm{fm}$.

JHEP 08 (2010) 071
PRD 95 (2017) 074504

Physical extrapolation (two-state summation, model 1)

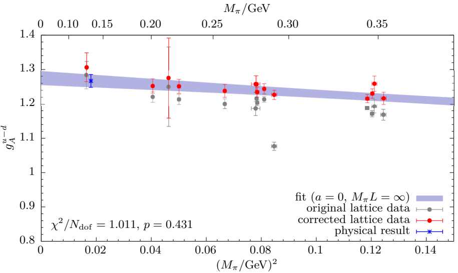

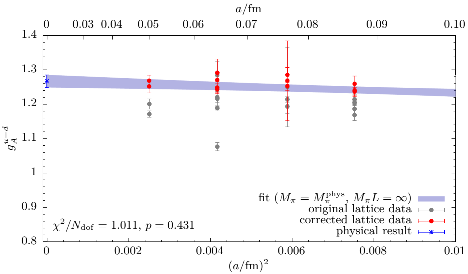

- Data are very well described by fit model 1.
- Chiral and continuum extrapolations are mild.
- Finite volume corrections can be sizable for small boxes. (already seen in 2019 analysis).
- Physical result $g_A^{u-d} = 1.267(18)_{\mathrm{stat}}$ in agreement with result on E250 and with experiment.

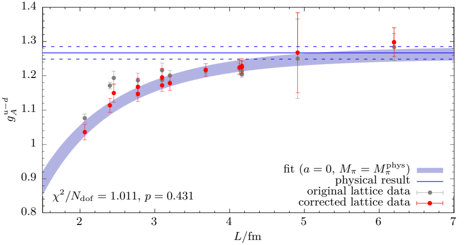

Physical extrapolation (two-state summation, model 2)

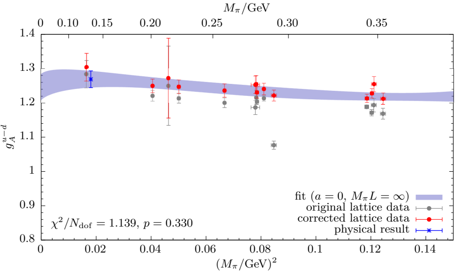

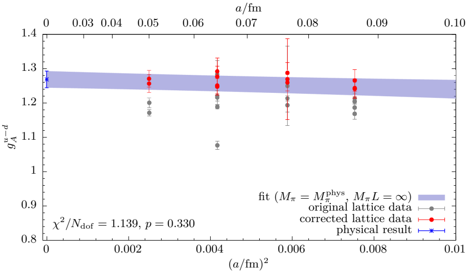

- NNLO fit (model 2) yields good description of data.
- Larger stat. errors due to additional fit parameter.
- Physical results from both fit models agree

$$g_A^{u-d} = 1.267(18)_{\mathrm{stat}} \quad \text{(fit 1)}$$
$$g_A^{u-d} = 1.269(24)_{\mathrm{stat}} \quad \text{(fit 2)}$$

- Will perform cuts (M_π, a, volume) to assign systematic errors in final analysis.

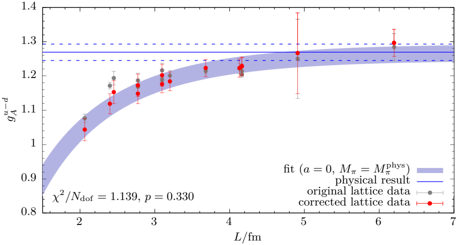

Plain summation vs. two-state summation physical results

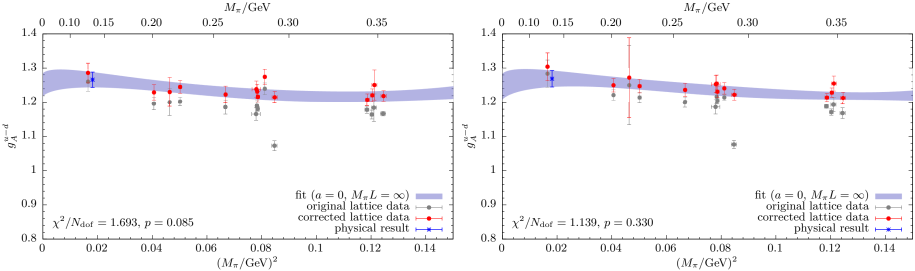

- Physical result for $g_A^{u-d} = 1.266(22)_{\mathrm{stat}}$ from plain summation method in good agreement with two-state procedure.
- Fit quality somewhat worse, might need even more conservative choice of $t_{\mathrm{sep}}^{\mathrm{min}}$'s in some cases.
- Fitting two-state model to data at $Q^2 \neq 0$ not feasible due to increased number of parameters and statistical precision.
- Obtaining a parametrization of the physical form factor requires a procedure that can be applied for any Q^2.

$\Rightarrow$ **Use plain summation method for $G_A^{u-d}(Q^2)$ data.**

Isovector axial form factor

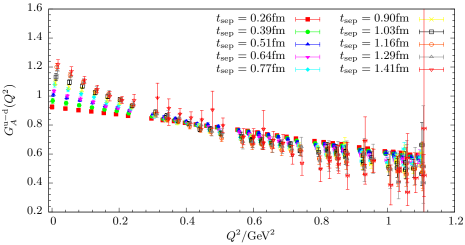

$M_\pi = 130\,\mathrm{MeV},\ a \approx 0.064\,\mathrm{fm},\ T/a \cdot (L/a)^3 = 192 \cdot 96^3$

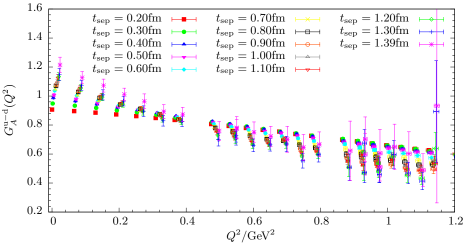

$M_\pi = 173\,\mathrm{MeV},\ a \approx 0.050\,\mathrm{fm},\ T/a \cdot (L/a)^3 = 192 \cdot 96^3$

- Large, fine boxes with (near) physical quark mass and high momentum resolution.
- Trend of excited state contamination reversed at around $Q^2 \approx 0.4\,\mathrm{GeV}^2$.
- Signal quality deteriorates at increasing Q^2.
- Data up $Q^2 \gtrsim 1\,\mathrm{GeV}^2$ available on all ensembles.

GOAL: Parametrization of physical G_A^{u-d} over large momentum range $0 \leq Q^2 \lesssim 1\,\mathrm{GeV}^2$.

Analysis strategy

Analysis of $G_A^{u-d}(Q^2)$ is carried out in several steps:

1. Compute effective FF $G_A^{u-d}(\vec{q}, t_{\rm sep}, t_{\rm ins})$ on each ensemble.
2. Extract groundstate $G_A^{u-d}(Q^2)$ using summation method:

$$S(Q^2, t_{\rm sep}) = \sum_{t=a}^{t_{\rm sep}-a} G_A^{u-d}(\vec{q}, t_{\rm sep}, t_{\rm ins}) = K(Q^2) + G_A^{u-d}(Q^2)(t_{\rm sep} - a) \ + \ \ldots$$

3. Use z-expansion to parametrize FF on each ensemble:

$$G_A^{u-d}(Q^2) = \sum_{n=0}^{N_z} c_n z^n, \quad z = \frac{\sqrt{t_{\rm cut} + Q^2} - \sqrt{t_{\rm cut} + Q^2}}{\sqrt{t_{\rm cut} - t_0} + \sqrt{t_{\rm cut} - t_0}},$$

   with $c_0 = g_A^{u-d}$, $c_1 \sim \langle r_A^2 \rangle$ and we choose $t_{\rm cut} = 9M_\pi^2$, $t_0 = 0$ and $N_z = 2$.

4. Perform physical extrapolation of coefficients $c_n \rightarrow$ parametrization of physical FF
5. Study of systematics.

Analysis: $t_{\rm sep}^{\rm min}$–dependence of c_n.

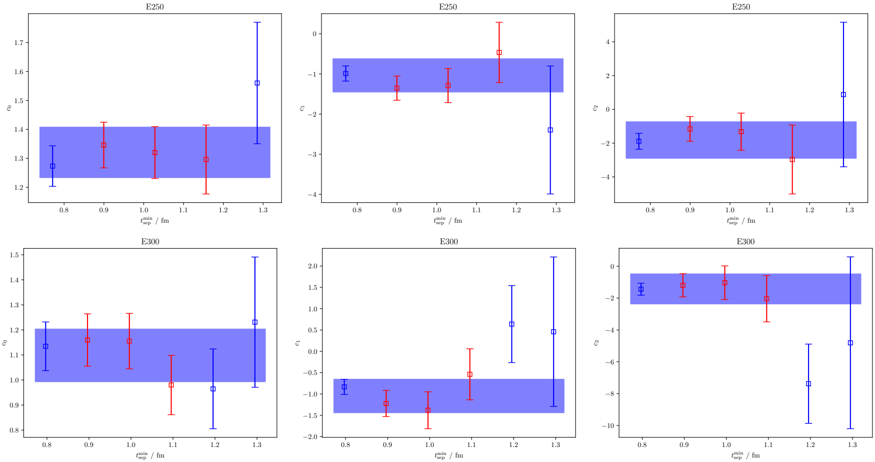

- Data typically less precise than results for g_A^{u-d} from dedicated analysis.
- Signal is lost for $t_{\rm sep}^{\rm min} \gtrsim 1\,{\rm fm}$, but fluctuations can still be significant for $t_{\rm sep}^{\rm min} < 1\,{\rm fm}$ (especially for $c_{1,2}$).

$\rightarrow$ **Make a conservative choice, i.e. average over three values for $t_{\rm sep}^{\rm min} \geq 0.8\,{\rm fm}$.**

Analysis: Physical extrapolation of c_n.

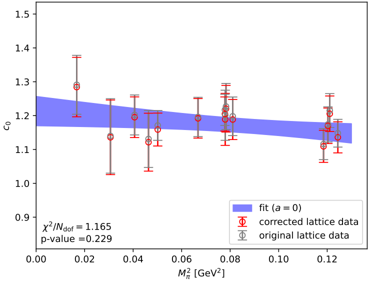

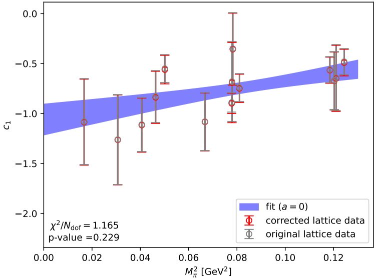

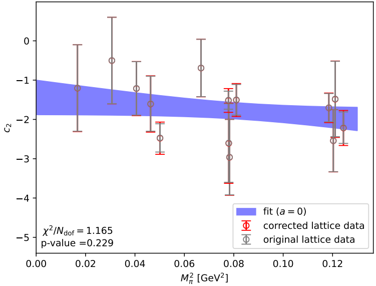

Two choices of fit model:

- Either use model 1 for all c_n...

Analysis: Physical extrapolation of c_n.

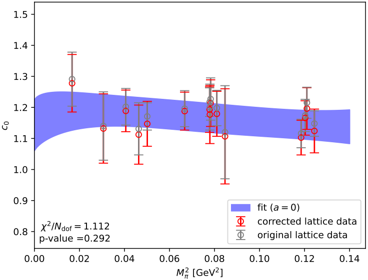

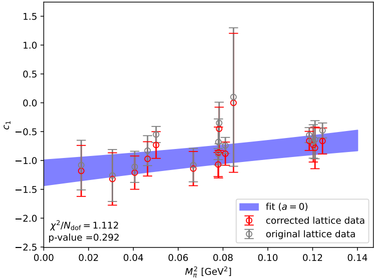

Two choices of fit model:

- Either use model 1 for all c_n...
- ... or use (NNLO) model 2 for c_0 and model 1 for $c_{1,2}$.

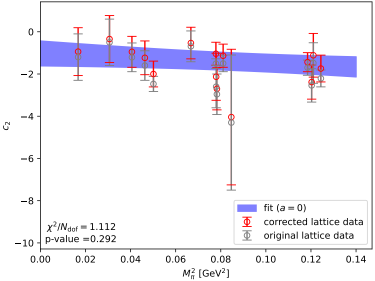

Analysis: Physical extrapolation of c_n.

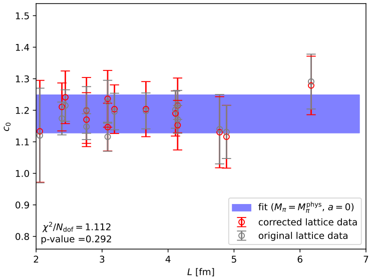

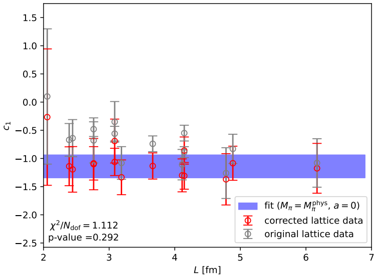

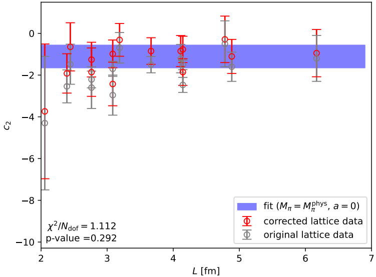

Two choices of fit model:

- Either use model 1 for all c_n...
- ... or use (NNLO) model 2 for c_0 and model 1 for $c_{1,2}$.

What about finite volume effects and continuum limit?

- Data not precise enough to resolve finite size correction.

Analysis: Physical extrapolation of c_n.

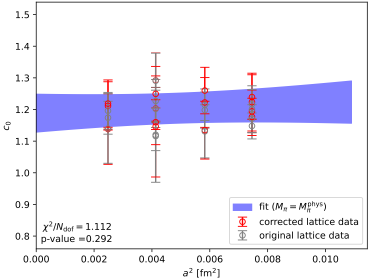

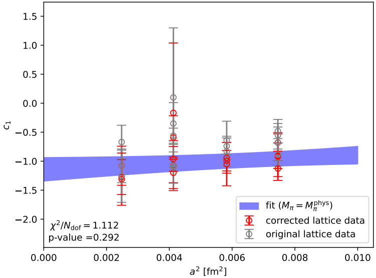

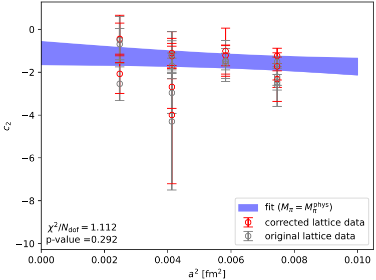

Two choices of fit model:

- Either use model 1 for all c_n...
- ... or use (NNLO) model 2 for c_0 and model 1 for $c_{1,2}$.

What about finite volume effects and continuum limit?

- Data not precise enough to resolve finite size correction.
- Mild continuum limit, but for $c_{1,2}$ priors might be needed for $\sim a^2$ term.

Physical form factor

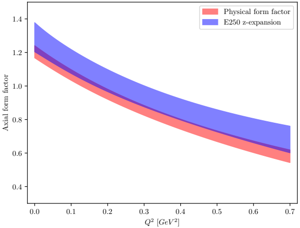

Fit model 1 for c_0

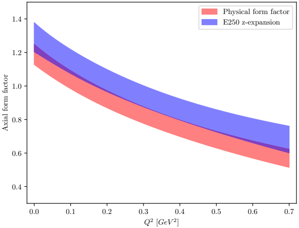

Fit model 2 for c_0

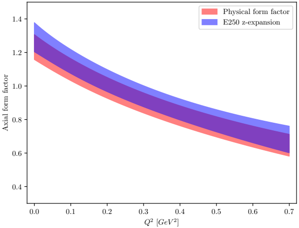

Fit model 2 for c_0, $M_\pi \lesssim 290\,\mathrm{MeV}$.

- Results for physical form factor close to most chiral ensemble.
- Pion mass cut increases c_0 and shift form factor upwards (but within errors).
- Implement further variations of the physical extrapolation to test for systematic effects. (e.g. fit 1 and fit 2 with and w/o finite volume term, cuts in M_π, a etc.)
- Use Akaike information criterion to assign a weight $\sim \exp\left(-\frac{1}{2}\left(\chi^2 + 2N_{\mathrm{param}} - N_{\mathrm{data}}\right)\right)$ to each fit.

H. Akaike, IEEE Transactions on Automatic Control 19, 716 (1974)

$\rightarrow$ **Perform model average and include systematic error.**

Model average and axial radius $\langle r_A^2 \rangle$

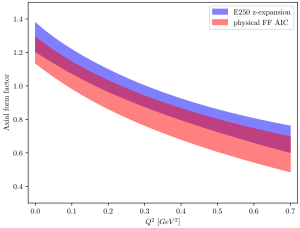

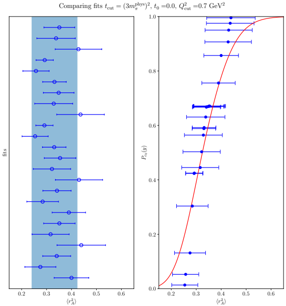

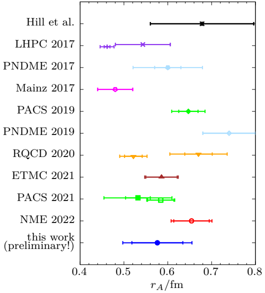

- Model average increases error.
- (Preliminary!) result for axial radius

$$\boxed{r_A = 0.574(59)_{\mathrm{stat}}(53)_{\mathrm{sys}}\,\mathrm{fm} = 0.574(79)\,\mathrm{fm}}$$

  compatible with other recent lattice determinations.
- Result for axial charge / c_0

$$\boxed{g_A^{u-d} = 1.214(72)_{\mathrm{stat}}(32)_{\mathrm{sys}} = 1.214(79)}$$

  smaller than result from dedicated analysis but compatible within factor ~ 4 larger errors.

Form factor comparison with experimental data

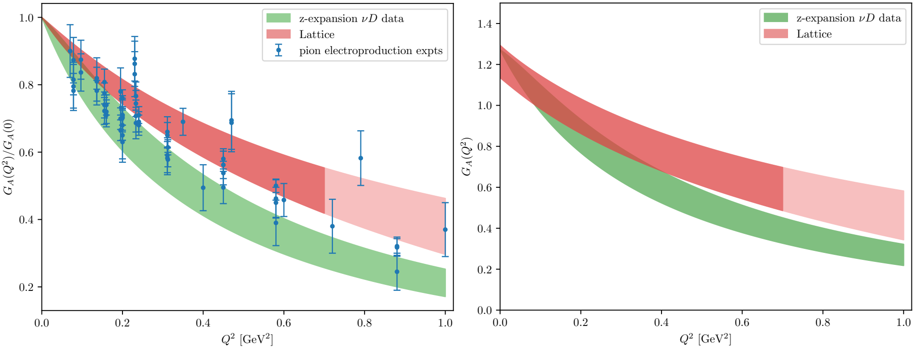

- Physical FF does not fully reproduce curvature of νD scattering data.
  (but in qualitative agreement with other lattice determinations)
- Effect slightly more pronounced for data normalized by g_A^{u-d}
- Some tension remains in the extrapolation, more restrivtive Q^2-cut, e.g. $Q^2 \leq 0.5\,\mathrm{GeV}^2$ might help, or including further coefficients in the z-expansion.
- Will provide results for coefficients c_n or rather the ratios c_1/c_0, c_2/c_0 and c_2/c_1 including errors and correlations in planned publication.

Summary and outlook

- Lattice calculation of axial form factor on large set of ensemble with $M_\pi \in [130\,\mathrm{MeV}, 350\,\mathrm{MeV}]$, four values of $a \in [0.050\,\mathrm{fm}, 0.086\,\mathrm{fm}]$ and $L \in [2\,\mathrm{fm}, 6\,\mathrm{fm}]$.

- Result(s) for g_A^{u-d} from dedicated analysis in excellent agreement with experimental value.

  $\rightarrow$ Result statistically precise, error $\lesssim 2\%$

  $\rightarrow$ **Excited states** and **physical extrapolation** well under control.

- Obtained parametrization of the physical isovector axial form factor G_A^{u-d}

  $\rightarrow$ **Excited states** tamed by summation method and controlled **physical extrapolation**.

  $\rightarrow$ Systematics due to extrapolations, different fit choices etc. taken into account by **model averaging**.

  $\rightarrow$ Results for r_A and curvature of form factor up to $\lesssim 1\,\mathrm{GeV}^2$ agrees with other lattice determinations.

- Additional plans / improvements:

  $\rightarrow$ Doubling statistics on E300 ($M_\pi = 172\,\mathrm{MeV}$, $a = 0.050\,\mathrm{fm}$) should further improve control over chiral and continuum extrapolations.

  $\rightarrow$ Further refine z-expansion ansatz and model averaging.

  $\rightarrow$ Quark-disconnected loop data available for all ensembles; could also study quark flavor decomposition.

Physical extrapolation (two-state summation, model 2, $M_\pi \lesssim 290\,\mathrm{MeV}$)

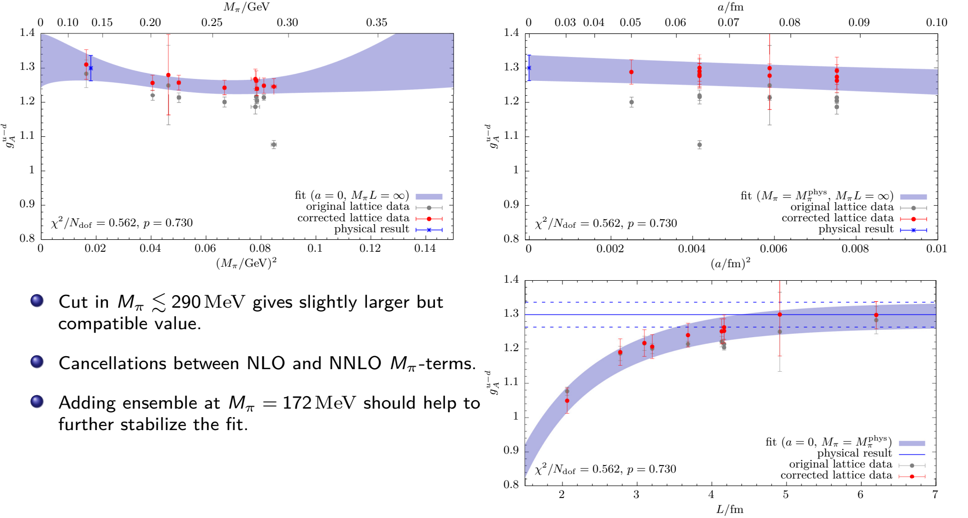

- Cut in $M_\pi \lesssim 290\,\mathrm{MeV}$ gives slightly larger but compatible value.
- Cancellations between NLO and NNLO M_π-terms.
- Adding ensemble at $M_\pi = 172\,\mathrm{MeV}$ should help to further stabilize the fit.